

Mechanistic Insights Into Hsp104 Potentiation

Mariana P. Torrente^{*,^}, Edward Chuang^{*,§}, Megan M. Noll^{*,‡}, Meredith E. Jackrel^{*,‡}, Michelle S. Go^{*,¶},
and James Shorter^{*,§}

From the ‡Department of Biochemistry and Biophysics and §Pharmacology Graduate Group, Perelman School of Medicine, University of Pennsylvania, Philadelphia, PA 19104. ^Present address: Chemistry Department of Brooklyn College and Ph.D. Programs in Chemistry, Biochemistry, and Biology, The Graduate Center of The City University of New York, New York, NY 10016. ¶Present address: Department of Medicine, University of North Carolina School of Medicine, Chapel Hill, NC 27599.

* Running Title: *Mechanistic Insights Into Hsp104 Potentiation*

To whom correspondence should be addressed: Prof. James Shorter, 805B Stellar-Chance Laboratories, 422 Curie Blvd., Philadelphia, PA 19104. Tel.: 215-573-4256; Fax: 215-898-9871; E-mail: jshorter@mail.med.upenn.edu

Keywords: Protein Disaggregase, Hsp104, Protein Engineering, TDP-43, FUS, α -synuclein

Potentiated variants of Hsp104, a protein disaggregase from yeast, can dissolve protein aggregates connected to neurodegenerative diseases such as Parkinson's disease and amyotrophic lateral sclerosis. However, the mechanisms underlying Hsp104 potentiation remain incompletely defined. Here, we establish that 2-3 subunits of the Hsp104 hexamer must bear an A503V potentiating mutation to elicit enhanced disaggregase activity in the absence of Hsp70. We also define the ATPase and substrate-binding modalities needed for potentiated Hsp104^{A503V} activity *in vitro* and *in vivo*. Hsp104^{A503V} disaggregase activity is strongly inhibited by the Y257A mutation that disrupts substrate binding to the nucleotide-binding domain 1 (NBD1) pore loop, and is abolished by the Y662A mutation that disrupts substrate binding to the NBD2 pore loop. Intriguingly, Hsp104^{A503V} disaggregase activity responds to mixtures of ATP and ATP γ S (a slowly hydrolyzable ATP analogue) differently than Hsp104. Indeed, an altered pattern of ATP hydrolysis and altered allosteric signaling between NBD1 and NBD2 are likely critical for potentiation. Hsp104^{A503V} variants bearing inactivating Walker A or Walker B mutations in both NBDs are inoperative. Unexpectedly, however, Hsp104^{A503V} retains potentiated activity upon introduction of sensor-1 mutations that reduce ATP hydrolysis at NBD1 (T317A) or NBD2 (N728A).

Hsp104^{T317A A503V} and Hsp104^{A503V N728A} rescue TDP-43, FUS, and α -synuclein toxicity in yeast. Thus, Hsp104^{A503V} displays a more robust activity that is unperturbed by sensor-1 mutations that greatly reduce Hsp104 activity *in vivo*. Indeed, ATPase activity at NBD1 or NBD2 is sufficient for Hsp104 potentiation. Our findings will empower design of ameliorated therapeutic disaggregases for various neurodegenerative diseases.

Protein misfolding and aggregation are associated with a wide variety of diseases, ranging from type II diabetes (1,2) to neurodegenerative diseases such as fatal familial insomnia (3,4), Parkinson's disease (PD) and amyotrophic lateral sclerosis (ALS) (5-7). In PD patients, α -synuclein (α -syn) forms toxic soluble oligomers as well as amyloid structures that accumulate in Lewy bodies and contribute to the death of dopaminergic neurons (8-12). Similarly, toxic soluble oligomers and cytoplasmic inclusions of TDP-43 or FUS are associated with ALS and frontotemporal dementia (13-20). These misfolded protein conformers are recalcitrant and represent a colossal roadblock in the treatment of these diseases.

Hsp104 is a 102kDa AAA+ ATPase (21) from *Saccharomyces cerevisiae* capable of dissolving disordered protein aggregates as well as dismantling amyloid fibrils and toxic soluble oligomers (22-33). It assembles into a

homo-hexameric barrel structure with a central channel (34-39). Hsp104 processes protein aggregates by directly translocating substrates either partially or completely through this channel (35,36,40-46). Hsp104 encompasses an N-terminal domain (NTD), two nucleotide-binding domains (NBD1 and NBD2), a coiled-coil middle domain (MD), and a C-terminal domain important for oligomerization (Fig. 1A) (47). Both NBDs contain Walker A and Walker B motifs that are critical for nucleotide binding and hydrolysis, respectively (48). ATP hydrolysis takes place primarily at NBD1, whereas NBD2 has a nucleotide-dependent oligomerization function (29,34,49-52).

Remarkably, Hsp104 can remodel amyloid substrates alone, without the aid of any other chaperones (22,24,26,31,33,45,53-56). However, to disaggregate amorphous protein aggregates, Hsp104 usually needs to collaborate with the Hsp110, Hsp70, and Hsp40 chaperone system (23,26,30,32,57). Moreover, small heat shock proteins such as Hsp26 can enhance disaggregase activity further (30,57-59). *In vitro*, mixtures of ATP and ATP γ S (a slowly hydrolyzable ATP analog) enable Hsp104 to dissolve amorphous aggregates in the absence of Hsp70 and Hsp40 (26,35,60,61).

Wild-type (WT) Hsp104 can resolve α -syn oligomers and fibrils, but very high Hsp104 concentrations are required (26,31,32). Hsp104 has limited disaggregase activity against TDP-43 and FUS fibrils (62,63). Recently, we have engineered potentiated Hsp104 variants that mitigate TDP-43, FUS, and α -syn misfolding (62-67). Missense mutations at disparate but specific positions in the MD or the small domain of NBD1 (immediately C-terminal to the MD) resulted in potentiated Hsp104 variants (62,67). Potentiating mutations in the MD obviate any absolute requirement for Hsp70 in disaggregation of amorphous aggregates and typically (under physiological salt conditions) enhance Hsp104 ATPase activity (62,67). Potentiated Hsp104 variants also display accelerated substrate translocation, enhanced unfoldase activity, and enhanced amyloid-remodeling activity (45,62). They can also recognize shorter unfolded tracts in client proteins compared to Hsp104 (63). Hsp104^{A503V} has been previously established as a potentiated Hsp104 variant able to ameliorate the

toxicity arising from the aggregation of WT or disease-linked forms of α -syn, FUS and TDP-43 in yeast (62,63). Hsp104^{A503V} hexamers also display enhanced plasticity and are more resistant to defective subunits than Hsp104 (62). However, Hsp104^{A503V} is more sensitive than Hsp104 to suramin, a small molecule inhibitor of Hsp104 ATPase activity (68). Interestingly, two potentiated Hsp104 variants, Hsp104^{A503S} and Hsp104^{Y257F A503V Y662F}, rescue neurodegeneration in the metazoan nervous system and hold promise as possible treatments for neurodegenerative disease (62,66).

Despite these advances, the molecular mechanisms underlying the potentiation of Hsp104 are incompletely understood. The NTD of Hsp104 is critical for Hsp104 potentiation as is motif 1 (helix 1 and a portion of helix 2) of the MD (35,47,67). Thus, deletion of these large regions precludes potentiation (35,67). However, beyond these domain requirements little else is known. Here, we explore how many A503V subunits are needed per hexamer to enable enhanced activity. We also determine which Hsp104 ATPase and substrate-binding modalities are important for potentiation both *in vitro* and *in vivo*. The mechanistic insights gleaned from our studies will enable further development of potentiated Hsp104 variants as therapeutics for various neurodegenerative diseases.

EXPERIMENTAL PROCEDURES

Materials. All chemicals were purchased from Sigma Aldrich (St. Louis, MO) unless otherwise specified. Creatine kinase was purchased from Roche Applied Science (Indianapolis, IN). Firefly luciferase was purchased from Sigma Aldrich. Luciferase Assay Reagent was purchased from Promega (Madison, WI). Hsp70 (Hsp72) and Hsp40 Hdj1 were purchased from Enzo Life Sciences (Farmingdale, NY).

Protein Expression and Purification. Sixteen Hsp104 variants: Hsp104, Hsp104^{Y257A}, Hsp104^{T317A}, Hsp104^{A503V}, Hsp104^{Y662A}, Hsp104^{N728A}, Hsp104^{K218T K620T}, Hsp104^{E285Q E687Q}, Hsp104^{Y257A Y662A}, Hsp104^{Y257A A503V}, Hsp104^{T317A A503V}, Hsp104^{Y662A A503V}, Hsp104^{N728A A503V}, Hsp104^{K218T A503V K620T}, Hsp104^{E285Q A503V E687Q}, and Hsp104^{Y257A A503V Y662A} were purified as reported

previously (52,61,69). Briefly, untagged Hsp104 was transformed into BL21-DE3 RIL cells (Agilent Technologies, Santa Clara, CA). Expression was induced at an OD_{600} of 0.4–0.6 with 1mM IPTG for 15–18h at 15°C. Cells were harvested via centrifugation (4,000rpm, 4°C, 20 minutes), resuspended in lysis buffer (50mM Tris-HCl, pH 8.0, 10mM $MgCl_2$, 2.5% glycerol (w/v), 2mM β -mercaptoethanol (Bio-Rad Laboratories, Hercules, CA), 5 μ M pepstatin A, and 1 Mini-complete EDTA free protease tablet per 50mL (Roche), and lysed by sonication. Cell debris was removed via centrifugation at 16,000rpm at 4°C for 20 minutes. The supernatant was applied to Affi-Gel Blue resin (Bio-Rad). Supernatant and resin were rotated at 4°C for 4 hours. Resin was then washed with wash buffer (50mM Tris-HCl, pH 8.0, 10mM $MgCl_2$, 100mM KCl, 2.5% glycerol (w/v), 2mM β -mercaptoethanol). Hsp104 was eluted with high-salt buffer (wash buffer plus 1M KCl). Hsp104 was then further purified by ResourceQ anion exchange chromatography using running buffer Q (20mM TrisHCl pH 8.0, 0.5mM EDTA, 5mM $MgCl_2$, 50mM NaCl) and eluted with a linear gradient of buffer Q+ (20mM Tris-HCl pH 8.0, 0.5mM EDTA, 5mM $MgCl_2$, 1M NaCl). Eluate was exchanged into storage buffer (40mM HEPES-KOH pH 7.4, 150mM KCl, 20mM $MgCl_2$, 10% glycerol, 1mM DTT), snap frozen and stored at -80°C. High salt storage buffer (40mM HEPES-KOH pH 7.4, 500mM KCl, 20mM $MgCl_2$, 10% glycerol, 1mM DTT), was used for storage of Hsp104^{A503V} and all other Hsp104 variants containing this mutation.

ATPase Assay. WT or mutant Hsp104 (0.25 μ M monomer) in ATPase buffer (20mM HEPES-KOH pH 7.4, 20mM NaCl and 10mM $MgCl_2$) was incubated for 10 minutes at 25°C in the presence of ATP (1mM) as noted (52). ATPase activity was assessed by the release of inorganic phosphate determined by using a malachite green phosphate detection kit (Innova Biosciences, Cambridge, UK).

Luciferase Disaggregation Assays. Luciferase reactivation was performed as described (23,61). To assemble aggregates, firefly luciferase (50 μ M) in luciferase refolding buffer (LRB, 25mM HEPES-KOH, 7.4, 150mM potassium acetate, 10mM magnesium acetate, 10mM DTT) with 6M

urea was incubated at 30°C for 20 minutes. Luciferase was then rapidly diluted 100-fold into LRB, divided into 100 μ L aliquots, snap frozen in liquid N_2 , and stored at -80°C. For reactivation assays, aggregated luciferase (50nM) was incubated with Hsp104 (1 μ M hexamer), plus 5mM ATP (or indicated ATP γ S and ATP ratio amounting to the same total) and an ATP regeneration system (10mM creatine phosphate, 0.5 μ M creatine kinase (Roche), 0.1mM ATP) for 90 minutes at 25°C. For some assays, Hsp70 (1 μ M) and Hsp40 (1 μ M; Enzo Life Sciences) were added. Luciferase activity was assessed by luminescence measured on a Safire² microplate reader (Tecan, Männedorf, Switzerland).

Subunit Doping Assay. Hsp104 was mixed with Hsp104^{A503V} in varying ratios to give a total concentration of 0.167 μ M Hsp104 hexamer, and the luciferase reactivation experiments were performed as described above. Hsp70 and Hsp40 were omitted for these experiments such that WT Hsp104 was inactive. Thus, under these conditions, we are certain that if the number of WT subunits per hexamer exceeds five then the hexamer is inactive. We employed the approach of Reinstein and colleagues to simulate the distribution of Hsp104 and Hsp104^{A503V} subunits within a given population of Hsp104 hexamers as described (26,61,62,70). Thus, we employed the binomial distribution:

$$P(x) = \binom{n}{x} p^x (1-p)^{n-x}$$

where P is the probability that a hexamer (therefore, $n=6$) contains x WT subunits and p is the probability that a WT subunit is incorporated (26,61,62,70). Experiments demonstrated that WT and A503V subunits have a similar probability of being incorporated into a hexamer (26,62). Consequently, p is calculated as the molar ratio of WT and A503V protein present:

$$p = \frac{Hsp104}{(Hsp104 + Hsp104_{A503V})}$$

Therefore, for any specified percentage of WT subunits the probability distribution of Hsp104^{A503V} hexamers containing 0, 1, 2, 3, 4, 5 or

6 WT subunits can be derived (Fig. 1B) (26,61,62,70). Activity versus p plots could then be generated assuming each A503V subunit makes an equal contribution to the total activity (one-sixth per subunit) (Fig. 1C) (26,61,62,70). Consequently, if subunits within the Hsp104^{A503V} hexamer operate independently then activity should decline in a linear manner upon incorporation of WT subunits (26,61,62,70). Conversely, if subunits are coupled then a specific number of WT subunits will be sufficient to eliminate activity (26,61,62,70). Thus, zero activity is assigned to hexamers that are in breach of a specific threshold number of WT subunits (26,61,62,70). In this way, we can generate activity versus p plots if we assume that 1 or more, 2 or more, 3 or more, 4 or more, or 5 or more WT subunits are required to eliminate activity (26,61,62,70).

To further model the observed inhibitory effect of WT Hsp104 subunits on Hsp104^{A503V} activity we employed the binomial distribution as above, but imposed an additional rule whereby WT subunits repress the activity of adjacent A503V subunits by a factor of r (26,35,62,71). Thus, we scored each subunit-subunit interface of every possible hetero-hexamer in each possible configuration as follows: interfaces were scored as $1/6$ if at an A503V:A503V junction, $r/6$ if at an A503V:WT junction, or 0 if at a WT:WT junction (26,62). Activity was then normalized to the predicted hetero-hexamer population as defined by the binomial distribution above (Fig. 1B) (26, 59).

Yeast strains, Media, and Plasmids. All yeast were W303a Δ hsp104 (*MATa*, *can1-100*, *his3-11,15*, *leu2-3,112*, *trp1-1*, *ura3-1*, *ade2-1*) (72). Yeast were grown in synthetic media lacking the appropriate components. Media was supplemented with 2% glucose, raffinose, or galactose. Vectors encoding TDP-43, FUS, and α -syn (pAG303GAL-TDP-43, pAG303GAL-FUS, and pAG303GAL- α -syn-GFP, respectively) were from A. Gitler (73-75). pRS416GAL-Hsp104 variants have been described previously (62). Hsp104 mutations were generated using QuikChange site-directed mutagenesis (Agilent Technologies, Santa Clara, CA) and confirmed by DNA sequencing.

Yeast Transformation and Spotting Assays. Yeast were transformed according to standard protocols

using polyethylene glycol and lithium acetate (76). For the spotting assays, yeast were grown to saturation overnight in raffinose supplemented dropout media at 30°C. Cultures were serially diluted 5-fold and spotted in duplicate onto synthetic dropout media containing glucose or galactose. Plates were analyzed after growth for 2-3 days at 30°C.

Western Blotting. Yeast were grown and induced in galactose-containing medium for 5 hours (TDP-43 and FUS) or 8 hours (α -syn-GFP). Cultures were normalized to an optical density of 0.6; 6mL of cells were then harvested and treated with 0.2M NaOH for 5 minutes at room temperature. Resulting cell pellets were resuspended in 100 μ L 1 \times SDS sample buffer and boiled. Cell lysates were separated using SDS-PAGE (4-20% gradient, Bio-Rad) and then transferred to a PVDF membrane (EMD Millipore, Billerica, MA). Membranes were blocked using LI-COR blocking buffer for 1 hour at room temperature. Primary antibody incubations were performed at 4°C overnight. Antibodies used were: rabbit anti-GFP polyclonal (Sigma Aldrich, Cat#G1544), rabbit anti-TDP-43 polyclonal (Proteintech, Chicago, IL, Cat #10782-2-AP), rabbit anti-FUS polyclonal (Bethyl Laboratories, Montgomery, TX, Cat#A300-302A), rabbit anti-Hsp104 polyclonal (Enzo Life Sciences, Cat#ADI-SPA-1040-F) and mouse anti-3-phosphoglycerate kinase (PGK) monoclonal (Novex, Frederick, MD, Cat#459250). Blots were processed using goat anti-mouse and anti-rabbit secondary antibodies from LI-COR Biosciences (Lincoln, NE) and imaged using an Odyssey Fc Imaging system (LI-COR Biosciences, Lincoln, NE).

RESULTS

Hsp104 hexamers must contain 2-3 A503V subunits for enhanced disaggregase activity. To gain insight into the mechanism of Hsp104 potentiation, we focused on Hsp104^{A503V} (Fig. 1A), which is among the strongest suppressors of α -syn, FUS, and TDP-43 toxicity in yeast (62,63,67). First, we explored the effects of WT Hsp104 subunits on the disaggregase activity of Hsp104^{A503V} hexamers. To do so, we exploited the strict requirement of Hsp104 for Hsp70 and Hsp40 to reactivate luciferase trapped in disordered aggregates in the presence of ATP (23,26). In the

absence of Hsp70 and Hsp40, Hsp104 reactivation activity is abolished (Fig. 1C) (23,26). By contrast, Hsp104^{A503V} displays robust luciferase reactivation activity in the absence of Hsp70 and Hsp40 (Fig. 1C) (62). Thus, under these conditions, we are certain that if the number of WT subunits per Hsp104 hexamer exceeds five then the hexamer is inactive. To determine how many A503V subunits per hexamer are required to elicit disaggregase activity in the absence of Hsp70 and Hsp40, we employed a mutant subunit doping strategy (26,70). Here, subunits are mixed to generate heterohexamer ensembles according to the binomial distribution (Fig. 1B) (26,70). We have previously demonstrated that Hsp104 and Hsp104^{A503V} assemble into dynamic hexamers that rapidly exchange subunits, ensuring statistical incorporation of individual subunits (Fig. 1B) (26,62). By applying different heterohexamer ensembles comprised of Hsp104 and Hsp104^{A503V} subunits to reactivate disordered luciferase aggregates, we can obtain a measure of how many A503V subunits per hexamer are required for disaggregase activity in the absence of Hsp70 (Fig. 1B, C) (26,29,61,62,70).

We assembled different heterohexamer ensembles of Hsp104^{A503V} and Hsp104^{WT} subunits (Fig. 1B) and assessed their luciferase reactivation activity (Fig. 1C). Incorporation of Hsp104 subunits into Hsp104^{A503V} hexamers caused a shallow curvilinear decline in luciferase disaggregase activity consistent with ~4-5 WT Hsp104 subunits being necessary to inactivate the Hsp104^{A503V} hexamer (Fig. 1C, compare blue markers to purple and light blue lines). If 4 WT subunits inactivate the Hsp104^{A503V} hexamer then 2 A503V subunits are not enough for activity (hence we need 3), and if 5 WT subunits inactivate the Hsp104^{A503V} hexamer then a single A503V subunit is insufficient for activity (hence we need 2). Thus, 2-3 Hsp104^{A503V} subunits per hexamer are required to dissolve disordered luciferase aggregates in the absence of Hsp70. Strikingly, we previously demonstrated that 2 Hsp104 subunits must be capable of interacting with Hsp70 to enable Hsp104-mediated disaggregation of luciferase in the presence of Hsp70 (61). Hence, it is interesting that at least 2 A503V subunits are needed to enable otherwise WT hexamers to disaggregate luciferase in the absence of Hsp70 (Fig. 1C). This finding indicates that A503V

subunits might mimic the conformation of Hsp70-activated, WT Hsp104 subunits. Moreover, this dose response curve (Fig. 1C) also suggests that Hsp104^{A503V} subunits do not stimulate the activity of adjacent WT Hsp104 subunits (26,62). Thus, a single Hsp104^{A503V} subunit is unable to potentiate an otherwise WT hexamer.

Interestingly, however, none of the theoretical curves exactly match the experimental data (Fig. 1C). Rather, the data falls mostly between the curves for 4 or 5 WT subunits being required to inhibit the activity of an Hsp104^{A503V} hexamer (Fig. 1C, compare blue markers to purple and light blue lines). However, we could model the observed behavior more precisely if we imposed rules whereby a WT subunit represses the activity of an adjacent A503V subunit by a factor of ~0.3 and is inactive if adjacent to another WT subunit (Fig. 1D, compare blue markers to purple line; see Materials and Methods).

Hsp104^{A503V} disaggregase activity is diminished by mutations that disrupt substrate binding to NBD pore loops. We next examined how Hsp104^{A503V} would respond to specific defects in substrate binding. Residues Y257 and Y662 are located in flexible pore loops located within each NBD and face the central channel through which substrate is translocated (Fig. 1A) (37,38,42-44). Each pore loop tyrosine engages substrate directly and mutating these residues to alanine results in severely reduced (Y257A) or abolished (Y662A) disaggregation activity (43,44). We introduced missense mutations Y257A, Y662A, or both in combination with A503V resulting in Hsp104^{A503V Y257A}, Hsp104^{A503V Y662A} and Hsp104^{A503V Y257A Y662A}. First, we measured the ATPase activity of these Hsp104 variants using the more sensitive low salt conditions of Hattendorf and Lindquist (52), which maximally stabilize Hsp104 hexamers. Under these conditions, surprisingly, Hsp104^{A503V} displays only ~18% higher ATPase activity than Hsp104 (Fig. 2A). Thus, enhanced ATPase activity of Hsp104^{A503V} compared to Hsp104 determined previously at physiological salt concentrations may reflect slight variations in hexamer stability (62,77,78). Hsp104 displayed similar ATPase activity to Hsp104^{Y257A} and Hsp104^{Y662A}, but Hsp104^{Y257A Y662A} ATPase activity was significantly elevated (Fig. 2A). We had not observed this increase previously at

physiological salt concentrations (26). Compared to Hsp104^{A503V}, Hsp104^{Y257A A503V} and Hsp104^{Y662A A503V} had very similar ATPase activity, whereas Hsp104^{Y257A A503V Y662A} was ~35% lower (Fig. 2A). Thus, the double pore loop mutation had opposite effects on ATPase activity in the wild type versus A503V background (Fig. 2A). Nonetheless, all pore-loop variants displayed robust ATPase activity under these conditions.

We next assessed the reactivation of luciferase trapped in disordered aggregates in the absence of Hsp70 and Hsp40, but in the presence of ATP. Under these conditions, Hsp104^{A503V} is ~33-fold more active than Hsp104 (Fig. 2B). In the A503V background, the pore loop mutations abolish this enhanced activity and reduce refolding activity to a low level similar to Hsp104 (Fig. 2B) (23). The effect of Y662A is slightly greater than Y257A, but either mutation severely diminishes Hsp104^{A503V} activity (Fig. 2B). Thus, Hsp104^{A503V} disaggregase activity is likely mediated via substrate interactions with Y257 and Y662.

In the presence of 1:1 mixtures of ATP and ATP γ S, Hsp104 can disaggregate disordered aggregates in the absence of Hsp70 (26,60,61,68). Under these conditions, Hsp104^{A503V} displays reduced luciferase reactivation activity compared to Hsp104 (Fig. 2C). This finding suggests that Hsp104^{A503V} responds differently than Hsp104 to mixtures of ATP and ATP γ S, which we explore further below. In these conditions, Hsp104^{Y257A} and Hsp104^{Y662A} are devoid of luciferase reactivation activity. Likewise, all pore-loop variants bearing the A503V mutation show diminished luciferase reactivation activity (Fig. 2C).

Next, we studied Hsp104 disaggregase activity in the presence of Hsp72 (an Hsp70) and Hdj1 (an Hsp40). Here, Hsp104^{A503V} luciferase-refolding activity is ~2-fold lower than Hsp104 (Fig. 2D). This result was surprising because Hsp104^{A503V} has increased luciferase reactivation activity in the presence of Hsc70 and Hdj2 as well as Sse1, Ssa1, and Ydj1 (62,67). Thus, the identity of Hsp70 and Hsp40 chaperone partners can modulate the activity of Hsp104^{A503V} differently than Hsp104. For both Hsp104 and Hsp104^{A503V}, Y257A or Y662A greatly reduced activity (Fig. 2D). The Y257A mutation greatly impairs activity in both Hsp104 and Hsp104^{A503V}, whereas the Y662A or the Y257A:Y662A mutations abolish

activity (Fig. 2D) (62). Thus, Y257 and Y662 play a crucial role in Hsp104^{A503V} disaggregase activity, indicating that potentiated Hsp104 variants employ a similar mechanism of substrate translocation to Hsp104.

To complement our *in vitro* studies, we utilized yeast models of cytotoxic misfolding and aggregation of proteins involved in neurodegenerative diseases such as PD and ALS (74,75,79). In PD, α -syn assembles into toxic soluble oligomers and amyloid fibrils (80). In yeast, expression α -syn from the galactose promoter induces cytoplasmic aggregation and toxicity (79). In these experiments, we exploited a *Δhsp104* yeast strain to avoid any potential interference from endogenous Hsp104 (Fig. 3A, B) (62). Deletion or overexpression of Hsp104 does not affect α -syn aggregation or toxicity in yeast (62,63,67). Thus, we can be certain that any rescue of toxicity by an Hsp104 variant in the *Δhsp104* background is due to a gain of Hsp104 therapeutic function (62,63,67). We first established differences in growth were not due to changes in the expression of α -syn or Hsp104 variants via immunoblotting (Fig. 3B). As expected, a vector control, Hsp104, Hsp104^{Y257A}, Hsp104^{Y662A} or Hsp104^{Y257A Y662A} did not reduce α -syn toxicity (Fig. 3A). By contrast, Hsp104^{A503V} strongly suppressed α -syn toxicity (Fig. 3A) (35,62,63,66). This rescue was severely impaired by the Y257A mutation and ablated by the Y662A or Y257A:Y662A mutations (Fig. 3A).

In ALS, the RNA-binding proteins with prion-like domains, TDP-43 or FUS, mislocalize from the nucleus and form cytoplasmic aggregates in degenerating motor neurons (17,18,80). In yeast, expression FUS or TDP-43 from the galactose promoter induces their cytoplasmic aggregation and toxicity (73-75). Here too, we utilized a *Δhsp104* yeast strain (Fig. 3D-F), in which FUS or TDP-43 aggregate and are highly toxic (62,73,81). Hsp104^{A503V} mitigates cytoplasmic FUS aggregation and toxicity in yeast, whereas Hsp104 has no effect (Fig. 3C) (35,62,63,66,81). This rescue is abrogated by the Y257A mutation (Fig. 3C). No other Hsp104 variant tested here reduced FUS toxicity (Fig. 3C). Consistent with previous reports (62,63), we found that Hsp104^{A503V} slightly reduced FUS expression levels (Fig. 3D). However, Hsp104^{A503V} was also

expressed at lower levels than the other Hsp104 variants (Fig. 3D).

None of the pore loop mutants could suppress TDP-43 toxicity in yeast (Fig. 3E) (62,73,74). Only Hsp104^{A503V} rescued TDP-43 toxicity (Fig. 3E). Hsp104^{A503V} very slightly reduced TDP-43 expression level and was itself also expressed at lower levels than Hsp104 (Fig. 3F). We conclude that the Hsp104 potentiation conferred by A503V is severely disrupted by the Y257A mutation and ablated by the Y662A mutation.

Hsp104^{A503V} responds differently than Hsp104 to mixtures of ATP and ATP γ S. Unlike Hsp104, Hsp104^{A503V} was not stimulated in luciferase reactivation by a 1:1 ratio of ATP to ATP γ S in the absence of Hsp70 (Fig. 2C). This finding suggested that an altered pattern of ATP hydrolysis by Hsp104^{A503V} hexamers might contribute to potentiation. To explore this idea further, we examined the effect of various ratios of ATP and ATP γ S on Hsp104 and Hsp104^{A503V} disaggregate activity. We kept the total adenine nucleotide concentration constant but varied the ATP:ATP γ S ratio. In Fig. 4A, we present the data normalized to WT Hsp104 maximal activity to reveal the amplitude of the activity of the different Hsp104 variants tested. In Fig. 4B, we present the data normalized to the maximal activity of each individual Hsp104 variant to reveal the optimal ATP:ATP γ S ratio. Hsp104 exhibited maximal luciferase reactivation activity at ~40-50% ATP γ S (Fig. 4A, B blue trace) (26,35). By contrast, the dose response of Hsp104^{A503V} was left shifted toward lower levels of ATP γ S (Fig. 4A, B compare blue and green traces). Thus, Hsp104^{A503V} exhibited maximal luciferase reactivation activity at ~20-30% ATP γ S (Fig. 4A, B green trace), and was sharply inhibited at ATP γ S concentrations that were optimal for Hsp104 (Fig. 4A, B). Utilization of ATP γ S in combination with ATP stimulates disaggregation of disordered aggregates by Hsp104 via slowing ATP hydrolysis at subset of nucleotide-binding sites (26,60). Thus, the heightened sensitivity of Hsp104^{A503V} to stimulation by lower proportions of ATP γ S indicates that Hsp104^{A503V} requires slowing of ATP hydrolysis at fewer nucleotide-binding sites than Hsp104.

ATP hydrolysis can be specifically slowed at NBD1 or NBD2 by mutating their conserved Walker A motif, which harbors a lysine residue that directly contacts the phosphates of ATP (21). Mutating the conserved lysine of the Walker A motif to threonine impairs ATP binding at that site (21,49,51). Alternatively, ATP hydrolysis can be slowed at NBD1 or NBD2 by mutating their conserved sensor-1 motif, which harbors a threonine or asparagine that interacts with the γ -phosphate of ATP (21,52). Mutating the conserved threonine or asparagine of the sensor-1 motif to alanine does not affect ATP binding but inhibits ATP hydrolysis at that site (21,52). Slowing ATPase activity specifically at NBD2 with K620T (Walker A) or N728A (sensor-1), but not NBD1 with K218T (Walker A) or T317A (sensor-1) (Fig. 1A), enables disaggregation of disordered aggregates by Hsp104 in the presence of ATP and absence of Hsp70 (Fig. 4A, B; data not shown) (60).

Next, we assessed how the disaggregate activity of the sensor-1 variants, Hsp104^{T317A} and Hsp104^{N728A}, was affected by increasing proportions of ATP γ S. Hsp104^{T317A} showed no disaggregate activity in the presence of just ATP (Fig. 4A, B black trace) (60). Surprisingly, however, mixtures of ATP and ATP γ S stimulated Hsp104^{T317A} disaggregate activity (Fig. 4A, B black trace). The dose response of Hsp104^{T317A} was similar to that of Hsp104 except slightly right shifted toward higher ATP γ S levels (Fig. 4A, B compare black and blue traces). Maximal Hsp104^{T317A} disaggregate activity was observed at ~50% ATP γ S, and at higher ATP γ S concentrations, Hsp104^{T317A} disaggregate activity declined (Fig. 4A, B compare black and blue traces). These findings indicate that, surprisingly, slowing ATP hydrolysis at NBD2 even when it is the only intact NBD can stimulate Hsp104 disaggregate activity against disordered aggregates in the absence of Hsp70.

In striking contrast, Hsp104^{N728A} maximally reactivates luciferase in the presence of ATP, but is sharply inhibited by increasing fractions of ATP γ S (Fig. 4A, B red trace) (60). This finding suggests that slowing ATP hydrolysis at NBD1 when it is the only intact NBD strongly inhibits disaggregate activity against disordered aggregates in the absence of Hsp70.

Hsp104^{T317A A503V} displayed a similar response to ATP γ S as Hsp104^{A503V} except that it was slightly right shifted toward higher ATP γ S levels (Fig. 4A, B compare orange and green traces). Indeed, Hsp104^{T317A A503V} was less inhibited than Hsp104^{A503V} by ATP γ S at concentrations higher than 30% (Fig. 4A, B compare orange and green traces). Maximal Hsp104^{T317A A503V} luciferase reactivation activity was observed at ~30% ATP γ S (Fig. 4A, B orange trace). Thus, the T317A mutation renders Hsp104 and Hsp104^{A503V} less sensitive to inhibition by higher ATP γ S concentrations.

Remarkably, Hsp104^{A503V N728A} was even more sensitive to inhibition by ATP γ S than Hsp104^{N728A} (Fig. 4A, B compare purple and red traces). Hsp104^{A503V N728A} maximally reactivates luciferase in the presence of ATP, but is completely inhibited by as little as 10% ATP γ S (Fig. 4A, B purple trace). Collectively, these observations indicate that altered ATP hydrolysis patterns might contribute to the enhanced activity of Hsp104^{A503V}. They also illustrate the startling mechanistic plasticity of the Hsp104 hexamer for disaggregating disordered aggregates (26).

Potentiated Hsp104^{A503V} activity can tolerate sensor-1 mutations in NBD1 or NBD2.

Hsp104^{A503V} exhibits increased ATPase activity at physiological salt concentrations (62,77,78) and is more sensitive to suramin, a small-molecule inhibitor of Hsp104 ATPase activity (68). Furthermore, we show here that Hsp104^{A503V} responds differently to ATP γ S (Fig. 4A, B). Moreover, Hsp104^{A503V} ATPase activity is inhibited and not stimulated by polylysine, unlike Hsp104 (78). These results suggest that altered ATPase activity is a key element enabling the potentiated activity of Hsp104^{A503V}. Thus, we next delineated the requirements for ATPase activity at NBD1 and NBD2 for potentiated Hsp104^{A503V} activity. To do so, we introduced the AAA+ sensor-1 mutations T317A and N728A (Fig. 1A) (52). We also introduced mutations in the Walker A and Walker B motifs of both NBDs; Hsp104^{K218T K620T} is unable to bind nucleotide while Hsp104^{E285Q E687Q} binds nucleotide, but it is unable to hydrolyze it (Fig. 1A) (82).

In the WT Hsp104 background, both sensor-1 mutants displayed significantly reduced ATPase activity, while the double Walker A and

Walker B mutants showed almost no activity (Fig. 5A) (49,51,52,82). Likewise, in the A503V background the double Walker A or double Walker B mutants eliminated ATPase activity (Fig. 5A). The NBD1 sensor-1 mutant displayed reduced ATPase activity in the A503V background (Fig. 5A, compared to Hsp104^{A503V}). Indeed, the ATPase activity of Hsp104^{T317A A503V} was reduced by ~32% compared to Hsp104^{A503V}, and this reduction was statistically significant (Fig. 5A). This reduction was similar to the effect of T317A in WT Hsp104 (Fig. 5A). By contrast, the activity of Hsp104^{A503V N728A} was reduced by only ~18% compared to Hsp104^{A503V}, and this reduction was not statistically significant (Fig. 5A). This reduction was not as large as the statistically significant ~33% reduction of ATPase activity caused by N728A in the WT Hsp104 background (Fig. 5A). However, we note that the ATPase activity of Hsp104^{T317A A503V} and Hsp104^{A503V N728A} were not significantly different (Fig. 5A). Collectively, these findings begin to suggest that allosteric communication between NBD1 and NBD2 may be altered in Hsp104^{A503V} (52,78). Indeed, NBD1 appears to make a larger contribution to the ATPase activity in Hsp104^{A503V} than in Hsp104 (Fig. 5A). These observations indicate that NBD1 may retain high ATPase activity when NBD2 is bound with ATP in the A503V background. By contrast, in Hsp104, NBD1 ATPase activity is low when ATP is bound by NBD2 (52).

Next, we determined the luciferase disaggregase activity of these Hsp104 ATPase variants in the presence of ATP but absence of Hsp70. In the presence of ATP alone, the double Walker A or Walker B mutants displayed insignificant luciferase reactivation activity in both the WT and A503V backgrounds (Fig. 5B). As expected, Hsp104 and Hsp104^{T317A} were also inactive in this setting (Fig. 5B). Hsp104^{A503V} and Hsp104^{T317A A503V} displayed robust disaggregase activity under these conditions (Fig. 5B). Thus, reducing ATPase activity at NBD1 did not affect the ability of Hsp104^{A503V} to disaggregate disordered aggregates. Hsp104^{N728A} reactivated luciferase trapped in urea-denatured aggregates ~11 fold more effectively than Hsp104^{A503V} (Fig. 5B). Although Hsp104^{N728A} has previously been shown to be active under these conditions (60), we were surprised that it was considerably more

active than Hsp104^{A503V}. Remarkably, Hsp104^{A503V N728A} displayed even greater luciferase reactivation activity (Fig. 5B). Thus, slowing ATP hydrolysis at NBD2 substantially enhances the ability of Hsp104 and Hsp104^{A503V} to disaggregate disordered aggregates in the presence of ATP and absence of Hsp70 (60).

In the presence of a 1:1 mixture of ATP:ATP γ S, the double Walker A or Walker B mutants were unable to elicit any luciferase reactivation in both the WT and A503V backgrounds (Fig. 5C). The T317A mutation had little effect on Hsp104 activity under these conditions, but slightly stimulated Hsp104^{A503V} activity (Fig. 4, 5C). By contrast, the N728A mutation strongly inhibited Hsp104 and Hsp104^{A503V} activity at 1:1 ATP:ATP γ S (Fig. 4, 5C). Thus, slowing ATP hydrolysis at NBD2 increases the sensitivity of Hsp104 and Hsp104^{A503V} to inhibition by ATP γ S.

In the presence of Hsp70 (Hsp72) and Hsp40 (Hdj1), the double Walker A or Walker B mutants were inactive in the WT and A503V background (Fig. 5D). Surprisingly, under these conditions, Hsp104^{T317A} activity was very similar to Hsp104, whereas Hsp104^{N728A} exhibited elevated activity (Fig. 5D). Similar results were observed in the A503V background. Thus, Hsp104^{T317A A503V} exhibited similar activity to Hsp104^{A503V}, whereas Hsp104^{A503V N728A} exhibited elevated activity, and was the most active variant in this assay (Fig. 5D). Under these conditions, slowing ATP hydrolysis at NBD2 increases Hsp104 and Hsp104^{A503V} luciferase reactivation activity in the presence of Hsp70 and Hsp40, whereas slowing ATP hydrolysis at NBD1 has little effect on activity (Fig. 5D). A summary of the various activities of the Hsp104 variants tested here is presented in Table 1.

Next, we assessed whether these Hsp104 ATPase variants could rescue toxicity of α -syn, FUS, or TDP-43 in yeast (Fig. 6A-F). In the context of WT Hsp104, none of the ATPase variants affected the expression or toxicity of α -syn (Fig. 6A, B), FUS (Fig. 6C, D), or TDP-43 (Fig. 6E, F) in yeast. Thus, despite having enhanced ability to reactivate luciferase aggregates *in vitro* (Fig. 5B, D), Hsp104^{N728A} was inactive against the neurodegenerative disease proteins *in vivo* (Fig. 6A, C, E). Previously, we had established that an important property of

potentiated Hsp104 variants bearing mutations in the MD was increased disaggregase activity against disordered aggregates in the absence of Hsp70 and Hsp40 (62,63,65-67). However, our findings with Hsp104^{N728A} (Fig. 5B, D, 6A, C, E) indicate that this activity is not sufficient for potentiated activity *in vivo*. Despite having enhanced ability to disaggregate disordered aggregates *in vitro* (Fig. 5B, D), Hsp104^{N728A} is unable to resolve amyloid conformers (24,33). By contrast, Hsp104^{A503V} has enhanced activity against both amyloid and non-amyloid aggregates *in vitro* (62,63,67). Thus, enhanced disaggregase activity against amyloid is a better predictor of potentiated activity *in vivo*.

Hsp104^{A503V} strongly rescued the toxicity of α -syn (Fig. 6A), FUS (Fig. 6C), and TDP-43 (Fig. 6E) in yeast (62,63,67). This potentiated activity was ablated by the double Walker A or Walker B mutations (Fig. 6A, C, E). Remarkably, however, both Hsp104^{T317A A503V} and Hsp104^{A503V N728A} retained potentiated activity *in vivo* and rescued toxicity of α -syn (Fig. 6A), FUS (Fig. 6C), and TDP-43 (Fig. 6E). Hsp104^{T317A A503V} rescued the toxicity of all three disease proteins just as well as Hsp104^{A503V} (Fig. 6A, C, E), whereas Hsp104^{A503V N728A} rescued α -syn and FUS toxicity just as well as Hsp104^{A503V} (Fig. 6A, C), but had reduced ability to rescue TDP-43 toxicity (Fig. 6E). Rescue of α -syn toxicity was observed without any effect on α -syn expression level (Fig. 6B). By contrast, rescue of FUS toxicity by Hsp104^{A503V} and Hsp104^{T317A A503V} was accompanied by a reduction in FUS expression level (Fig. 6D). However, Hsp104^{A503V N728A} rescued FUS toxicity without affecting FUS expression level (Fig. 6D). Hence, the reduction of FUS expression is not required to rescue toxicity. For TDP-43, Hsp104^{A503V} and Hsp104^{T317A A503V} also modestly reduced TDP-43 expression level, whereas Hsp104^{A503V N728A} did not (Fig. 6F). Therefore, the reduction in TDP-43 expression is also not required for rescue of toxicity. These findings suggest that the potentiated activity of Hsp104^{A503V} in yeast is largely unaffected by reducing ATPase activity at NBD1 or NBD2.

DISCUSSION

Several missense mutations at specific, but disparate positions in the MD or the small domain of NBD1 result in potentiated Hsp104 variants,

able to dissolve protein aggregates implicated in neurodegenerative diseases (35,62-67). These mutations likely disrupt a fragilely constrained, auto-inhibited state of Hsp104 (67). However, the exact molecular basis of Hsp104 potentiation remains unclear. Here, we have dissected mechanistic aspects of a potentiated Hsp104 variant, Hsp104^{A503V} (35,62-67). We have revealed how many subunits within the Hsp104 hexamer must bear a potentiating mutation to yield enhanced activity. We have also determined the ATPase and substrate-binding modalities that underpin potentiation *in vitro* and *in vivo*.

Using a mutant subunit doping strategy (26,35,61,70), we have established that 2-3 subunits of an otherwise WT hexamer must bear A503V mutations to elicit enhanced disaggregase activity in the absence of Hsp70. Intriguingly, at least two Hsp104 subunits must interact with Hsp70 to enable disaggregation of disordered aggregates (61). We suggest that A503V subunits mimic the conformation of WT Hsp104 subunits that have been activated by Hsp70 binding. Hsp70 and Hsp40 are often sequestered in disease-associated aggregates, which might inhibit their function (83,84). Thus, the ability of Hsp104^{A503V} to operate without Hsp70 and Hsp40 likely contributes to enhanced activity against disease-associated substrates in yeast (62,63,66,67). Nonetheless, the NBD2 sensor-1 variant, Hsp104^{N728A}, can disaggregate disordered aggregates (but not amyloid) *in vitro* in the absence of Hsp70 (24,33,60), but in contrast to Hsp104^{A503V}, Hsp104^{N728A} is unable to rescue α -syn, FUS, and TDP-43 toxicity in yeast. It is possible that Hsp104^{N728A} ATPase activity is too low to process certain aggregated substrates *in vivo*, or that there are elements inhibiting activity *in vivo* that we do not reconstitute in our *in vitro* experiments. Regardless, these findings suggest that separation from Hsp70 and Hsp40 is not the only important determinant in Hsp104 potentiation.

We show that the Hsp104 potentiation conferred by A503V is severely impaired by mutating conserved substrate-binding tyrosines to alanine. In WT Hsp104, mutating Y257 and Y662 to alanine results in severely reduced (Y257A) or abolished (Y662A) disaggregation activity (43,44). This was also the case for Hsp104^{A503V}. Hsp104^{Y257A A503V} retained slightly more activity

than Hsp104^{A503V Y662A} in all conditions tested *in vitro*. However, the Y257A pore-loop variants are unable to rescue yeast proteinopathy models. These results suggest that Hsp104^{A503V} recognizes and translocates substrates via direct contact with conserved Y257 and Y662 pore-loop residues in a manner similar to Hsp104.

In the absence of Hsp70, Hsp104^{A503V} disaggregase activity against disordered aggregates responded differently than Hsp104 to mixtures of ATP and ATP γ S. Indeed, optimal Hsp104^{A503V} disaggregase activity was observed at ~4:1 ATP:ATP γ S compared to ~1:1 for Hsp104. Mixtures of ATP γ S and ATP stimulate disaggregation of disordered aggregates by Hsp104 via decelerating ATP hydrolysis at a subset of nucleotide-binding sites (26,60). Thus, stimulation of disaggregase activity by lower fractions of ATP γ S indicates that Hsp104^{A503V} requires decelerated ATPase activity at fewer nucleotide-binding sites. This finding suggests that an altered pattern of ATP hydrolysis underlies Hsp104 potentiation.

Analysis of various ATPase-defective mutants revealed that enhanced Hsp104^{A503V} activity requires ATPase activity, as double Walker A or Walker B mutants were ATPase-dead and non-functional in all assays studied here (62). Interestingly, the sensor-1 mutants, T317A and N728A (52), revealed alterations in allosteric signaling between NBD1 and NBD2 in Hsp104^{A503V}. In the WT background both T317A and N728A significantly reduce Hsp104 ATPase activity (52). Indeed, based on this observation it is suggested that Hsp104 NBD1 ATPase activity is low when ATP is bound by NBD2 (52). However, in Hsp104^{A503V} only the T317A mutation significantly impairs ATPase activity. Indeed, N728A has little effect on Hsp104^{A503V} ATPase activity. It should be noted that despite these differences, the ATPase activity of Hsp104^{T317A A503V} and Hsp104^{A503V N728A} were not significantly different. Nonetheless, collectively, our findings begin to suggest that NBD1 makes a larger contribution to ATPase activity in Hsp104^{A503V} than in Hsp104. The essentially unaltered ATPase activity of Hsp104^{A503V N728A} may indicate that NBD1 retains high ATPase activity when NBD2 is bound with ATP in the A503V background. We suggest that this alteration in allosteric signaling

between NBD1 and NBD2 likely plays an important role in Hsp104 potentiation.

Remarkably, both Hsp104^{T317A A503V} and Hsp104^{A503V N728A} retain potentiated activity *in vivo* and *in vitro*. Thus, the potentiated activity of Hsp104^{A503V} is largely unaffected by reducing ATPase activity at NBD1 or NBD2. Hsp104^{A503V N728A} displayed slightly reduced ability to rescue TDP-43 toxicity in yeast, but still provided significant rescue. By contrast, the equivalent sensor-1 mutations in WT Hsp104 greatly reduce activity in yeast with respect to thermotolerance and prion propagation (52,85). Thus, Hsp104^{A503V} displays a more robust activity with an operational plasticity that is unperturbed by mutations that greatly reduce activity of Hsp104 *in vivo* (52,62,85). A summary of the key findings of our study is presented in Figure 7.

These insights into the molecular underpinnings of Hsp104 potentiation help to lay foundations to further develop next generation Hsp104 variants with ameliorated therapeutic utility for neurodegenerative diseases. For example, our findings hint that the specificity of potentiated Hsp104 variants might be sharpened by more subtle alterations to the NBD1 pore-loop or by more severely reducing NBD2 ATPase activity. Potentiated Hsp104 variants with enhanced substrate or conformer selectivity might exhibit reduced off-target effects and consequently display increased therapeutic efficacy and safety (66).

ACKNOWLEDGEMENTS

We thank Prof. Susan Lindquist, Prof. Aaron Gitler, and Dr. Morgan DeSantis for kindly sharing reagents. We thank Korrie Mack, Michael Soo, and Zachary March for helpful review of this manuscript. M.P.T was supported by a PENN-PORT postdoctoral fellowship (K12GM081259) and an NINDS Advanced Postdoctoral Career Transition Award (K22NS09131401) from the NIH; E.C. was supported by a Predoctoral Training Grant in Pharmacology (T32GM008076); M.E.J was supported by an American Heart Association Post-Doctoral Fellowship and a Target ALS Springboard Fellowship, and J.S. was supported by an NIH Director's New Innovator Award DP2OD002177, NIH grant R01GM099836, a Muscular Dystrophy

Association Research Award (MDA277268), Packard Center for ALS Research at Johns Hopkins University, and Target ALS.

CONFLICT OF INTEREST

The authors declare that they have no conflicts of interest with the contents of this article.

AUTHOR CONTRIBUTIONS

M.P.T. conceived and co-ordinated the study, designed, performed and analyzed the experiments shown in Fig. 2, 3, 4, 5, and 6, generated Fig. 1A and 7, and wrote the manuscript. E.C. designed, performed and analyzed the experiments shown in Fig. 2, 4, and 5. M.M.N. performed and analyzed the experiments shown in Fig. 3 and 6. M.E.J. conceived, designed, performed, and analyzed the experiment shown in Fig. 1B-D and prepared reagents used in Fig. 2, 4, and 5. M.S.G. contributed essential unpublished data, analysis, and interpretation for Fig. 2. J.S. conceived, coordinated, and directed the study and wrote the paper. All authors reviewed the results and approved the final version of the manuscript.

REFERENCES

1. Hoppener, J. W., Ahren, B., and Lips, C. J. (2000) Islet amyloid and type 2 diabetes mellitus. *N Engl J Med* **343**, 411-419
2. Kaniuk, N. A., Kiraly, M., Bates, H., Vranic, M., Volchuk, A., and Brumell, J. H. (2007) Ubiquitinated-protein aggregates form in pancreatic beta-cells during diabetes-induced oxidative stress and are regulated by autophagy. *Diabetes* **56**, 930-939
3. Capellari, S., Strammiello, R., Saverioni, D., Kretzschmar, H., and Parchi, P. (2011) Genetic Creutzfeldt-Jakob disease and fatal familial insomnia: insights into phenotypic variability and disease pathogenesis. *Acta Neuropathol* **121**, 21-37
4. Prusiner, S. B. (1998) The prion diseases. *Brain Pathol* **8**, 499-513
5. Forman, M. S., Trojanowski, J. Q., and Lee, V. M. (2004) Neurodegenerative diseases: a decade of discoveries paves the way for therapeutic breakthroughs. *Nat Med* **10**, 1055-1063
6. Ross, C. A., and Poirier, M. A. (2004) Protein aggregation and neurodegenerative disease. *Nat Med* **10 Suppl**, S10-17
7. Lansbury, P. T., and Lashuel, H. A. (2006) A century-old debate on protein aggregation and neurodegeneration enters the clinic. *Nature* **443**, 774-779
8. Spillantini, M. G., Schmidt, M. L., Lee, V. M., Trojanowski, J. Q., Jakes, R., and Goedert, M. (1997) Alpha-synuclein in Lewy bodies. *Nature* **388**, 839-840
9. Dawson, T. M., and Dawson, V. L. (2003) Molecular pathways of neurodegeneration in Parkinson's disease. *Science* **302**, 819-822
10. Luk, K. C., Kehm, V., Carroll, J., Zhang, B., O'Brien, P., Trojanowski, J. Q., and Lee, V. M. (2012) Pathological alpha-synuclein transmission initiates Parkinson-like neurodegeneration in nontransgenic mice. *Science* **338**, 949-953
11. Mahul-Mellier, A. L., Vercautere, F., Maco, B., Ait-Bouziad, N., De Roo, M., Muller, D., and Lashuel, H. A. (2015) Fibril growth and seeding capacity play key roles in alpha-synuclein-mediated apoptotic cell death. *Cell Death Differ* **22**, 2107-2122
12. Lashuel, H. A., Hartley, D., Petre, B. M., Walz, T., and Lansbury, P. T., Jr. (2002) Neurodegenerative disease: amyloid pores from pathogenic mutations. *Nature* **418**, 291
13. Robberecht, W., and Philips, T. (2013) The changing scene of amyotrophic lateral sclerosis. *Nat Rev Neurosci* **14**, 248-264
14. Fang, Y. S., Tsai, K. J., Chang, Y. J., Kao, P., Woods, R., Kuo, P. H., Wu, C. C., Liao, J. Y., Chou, S. C., Lin, V., Jin, L. W., Yuan, H. S., Cheng, I. H., Tu, P. H., and Chen, Y. R. (2014) Full-length TDP-43 forms toxic amyloid oligomers that are present in frontotemporal lobar dementia-TDP patients. *Nat Commun* **5**, 4824
15. Feiler, M. S., Strobel, B., Freischmidt, A., Hefnerich, A. M., Kappel, J., Brewer, B. M., Li, D., Thal, D. R., Walther, P., Ludolph, A. C., Danzer, K. M., and Weishaupt, J. H. (2015) TDP-43 is intercellularly transmitted across axon terminals. *J Cell Biol* **211**, 897-911
16. Kao, P. F., Chen, Y. R., Liu, X. B., DeCarli, C., Seeley, W. W., and Jin, L. W. (2015) Detection of TDP-43 oligomers in frontotemporal lobar degeneration-TDP. *Ann Neurol* **78**, 211-221
17. King, O. D., Gitler, A. D., and Shorter, J. (2012) The tip of the iceberg: RNA-binding proteins with prion-like domains in neurodegenerative disease. *Brain Res* **1462**, 61-80
18. Li, Y. R., King, O. D., Shorter, J., and Gitler, A. D. (2013) Stress granules as crucibles of ALS pathogenesis. *J Cell Biol* **201**, 361-372
19. Neumann, M., Sampathu, D. M., Kwong, L. K., Truax, A. C., Micsenyi, M. C., Chou, T. T., Bruce, J., Schuck, T., Grossman, M., Clark, C. M., McCluskey, L. F., Miller, B. L., Masliah, E., Mackenzie, I. R., Feldman, H., Feiden, W., Kretzschmar, H. A., Trojanowski, J. Q., and Lee, V. M. (2006) Ubiquitinated TDP-43 in frontotemporal lobar degeneration and amyotrophic lateral sclerosis. *Science* **314**, 130-133
20. Mackenzie, I. R., Rademakers, R., and Neumann, M. (2010) TDP-43 and FUS in amyotrophic lateral sclerosis and frontotemporal dementia. *Lancet Neurol* **9**, 995-1007

21. Hanson, P. I., and Whiteheart, S. W. (2005) AAA+ proteins: have engine, will work. *Nat Rev Mol Cell Biol* **6**, 519-529
22. DeSantis, M. E., and Shorter, J. (2012) Hsp104 drives "protein-only" positive selection of Sup35 prion strains encoding strong [PSI(+)]. *Chem Biol* **19**, 1400-1410
23. Glover, J. R., and Lindquist, S. (1998) Hsp104, Hsp70, and Hsp40: a novel chaperone system that rescues previously aggregated proteins. *Cell* **94**, 73-82
24. Shorter, J., and Lindquist, S. (2004) Hsp104 catalyzes formation and elimination of self-replicating Sup35 prion conformers. *Science* **304**, 1793-1797
25. Shorter, J. (2008) Hsp104: a weapon to combat diverse neurodegenerative disorders. *Neurosignals* **16**, 63-74
26. DeSantis, M. E., Leung, E. H., Sweeny, E. A., Jackrel, M. E., Cushman-Nick, M., Neuhaus-Follini, A., Vashist, S., Sochor, M. A., Knight, M. N., and Shorter, J. (2012) Operational Plasticity Enables Hsp104 to Disaggregate Diverse Amyloid and Nonamyloid Clients. *Cell* **151**, 778-793
27. Parsell, D. A., Kowal, A. S., Singer, M. A., and Lindquist, S. (1994) Protein disaggregation mediated by heat-shock protein Hsp104. *Nature* **372**, 475-478
28. Vashist, S., Cushman, M., and Shorter, J. (2010) Applying Hsp104 to protein-misfolding disorders. *Biochem Cell Biol* **88**, 1-13
29. Sweeny, E. A., and Shorter, J. (2015) Mechanistic and Structural Insights into the Prion-Disaggregase Activity of Hsp104. *J Mol Biol*
30. Duennwald, M. L., Echeverria, A., and Shorter, J. (2012) Small heat shock proteins potentiate amyloid dissolution by protein disaggregases from yeast and humans. *PLoS Biol* **10**, e1001346
31. Lo Bianco, C., Shorter, J., Regulier, E., Lashuel, H., Iwatsubo, T., Lindquist, S., and Aebischer, P. (2008) Hsp104 antagonizes alpha-synuclein aggregation and reduces dopaminergic degeneration in a rat model of Parkinson disease. *J Clin Invest* **118**, 3087-3097
32. Shorter, J. (2011) The mammalian disaggregase machinery: Hsp110 synergizes with Hsp70 and Hsp40 to catalyze protein disaggregation and reactivation in a cell-free system. *PLoS One* **6**, e26319
33. Shorter, J., and Lindquist, S. (2006) Destruction or potentiation of different prions catalyzed by similar Hsp104 remodeling activities. *Mol Cell* **23**, 425-438
34. Parsell, D. A., Kowal, A. S., and Lindquist, S. (1994) *Saccharomyces cerevisiae* Hsp104 protein. Purification and characterization of ATP-induced structural changes. *J Biol Chem* **269**, 4480-4487
35. Sweeny, E. A., Jackrel, M. E., Go, M. S., Sochor, M. A., Razzo, B. M., DeSantis, M. E., Gupta, K., and Shorter, J. (2015) The Hsp104 N-terminal domain enables disaggregase plasticity and potentiation. *Mol Cell* **57**, 836-849
36. Wendler, P., Shorter, J., Plisson, C., Cashikar, A. G., Lindquist, S., and Saibil, H. R. (2007) Atypical AAA+ subunit packing creates an expanded cavity for disaggregation by the protein-remodeling factor Hsp104. *Cell* **131**, 1366-1377
37. Carroni, M., Kummer, E., Oguchi, Y., Wendler, P., Clare, D. K., Sinning, I., Kopp, J., Mogk, A., Bukau, B., and Saibil, H. R. (2014) Head-to-tail interactions of the coiled-coil domains regulate ClpB activity and cooperation with Hsp70 in protein disaggregation. *Elife* **3**, e02481
38. Wendler, P., Shorter, J., Snead, D., Plisson, C., Clare, D. K., Lindquist, S., and Saibil, H. R. (2009) Motor mechanism for protein threading through Hsp104. *Mol Cell* **34**, 81-92
39. Lee, S., Sielaff, B., Lee, J., and Tsai, F. T. (2010) CryoEM structure of Hsp104 and its mechanistic implication for protein disaggregation. *Proc Natl Acad Sci U S A* **107**, 8135-8140
40. Shorter, J., and Lindquist, S. (2005) Navigating the ClpB channel to solution. *Nat Struct Mol Biol* **12**, 4-6
41. Weibezahn, J., Tessarz, P., Schlieker, C., Zahn, R., Maglica, Z., Lee, S., Zentgraf, H., Weber-Ban, E. U., Dougan, D. A., Tsai, F. T., Mogk, A., and Bukau, B. (2004) Thermotolerance requires

- refolding of aggregated proteins by substrate translocation through the central pore of ClpB. *Cell* **119**, 653-665
42. Tessarz, P., Mogk, A., and Bukau, B. (2008) Substrate threading through the central pore of the Hsp104 chaperone as a common mechanism for protein disaggregation and prion propagation. *Mol Microbiol* **68**, 87-97
 43. Lum, R., Niggemann, M., and Glover, J. R. (2008) Peptide and protein binding in the axial channel of Hsp104. Insights into the mechanism of protein unfolding. *J Biol Chem* **283**, 30139-30150
 44. Lum, R., Tkach, J. M., Vierling, E., and Glover, J. R. (2004) Evidence for an unfolding/threading mechanism for protein disaggregation by *Saccharomyces cerevisiae* Hsp104. *J Biol Chem* **279**, 29139-29146
 45. Castellano, L. M., Bart, S. M., Holmes, V. M., Weissman, D., and Shorter, J. (2015) Repurposing Hsp104 to Antagonize Seminal Amyloid and Counter HIV Infection. *Chem Biol* **22**, 1074-1086
 46. Li, T., Weaver, C. L., Lin, J., Duran, E. C., Miller, J. M., and Lucius, A. L. (2015) *Escherichia coli* ClpB is a non-processive polypeptide translocase. *Biochem J* **470**, 39-52
 47. DeSantis, M. E., and Shorter, J. (2012) The elusive middle domain of Hsp104 and ClpB: location and function. *Biochim Biophys Acta* **1823**, 29-39
 48. Franzmann, T. M., Czekalla, A., and Walter, S. G. (2011) Regulatory circuits of the AAA+ disaggregase Hsp104. *J Biol Chem* **286**, 17992-18001
 49. Schirmer, E. C., Queitsch, C., Kowal, A. S., Parsell, D. A., and Lindquist, S. (1998) The ATPase activity of Hsp104, effects of environmental conditions and mutations. *J Biol Chem* **273**, 15546-15552
 50. Grimminger-Marquardt, V., and Lashuel, H. A. (2010) Structure and function of the molecular chaperone Hsp104 from yeast. *Biopolymers* **93**, 252-276
 51. Schirmer, E. C., Ware, D. M., Queitsch, C., Kowal, A. S., and Lindquist, S. L. (2001) Subunit interactions influence the biochemical and biological properties of Hsp104. *Proc Natl Acad Sci U S A* **98**, 914-919
 52. Hattendorf, D. A., and Lindquist, S. L. (2002) Cooperative kinetics of both Hsp104 ATPase domains and interdomain communication revealed by AAA sensor-1 mutants. *EMBO J* **21**, 12-21
 53. Narayanan, S., Walter, S., and Reif, B. (2006) Yeast prion-protein, sup35, fibril formation proceeds by addition and subtraction of oligomers. *Chembiochem* **7**, 757-765
 54. Liu, Y. H., Han, Y. L., Song, J., Wang, Y., Jing, Y. Y., Shi, Q., Tian, C., Wang, Z. Y., Li, C. P., Han, J., and Dong, X. P. (2011) Heat shock protein 104 inhibited the fibrillization of prion peptide 106-126 and disassembled prion peptide 106-126 fibrils in vitro. *Int J Biochem Cell Biol* **43**, 768-774
 55. Shorter, J., and Lindquist, S. (2008) Hsp104, Hsp70 and Hsp40 interplay regulates formation, growth and elimination of Sup35 prions. *EMBO J* **27**, 2712-2724
 56. Sweeny, E. A., and Shorter, J. (2008) Prion proteostasis: Hsp104 meets its supporting cast. *Prion* **2**, 135-140
 57. Torrente, M. P., and Shorter, J. (2013) The metazoan protein disaggregase and amyloid depolymerase system: Hsp110, Hsp70, Hsp40, and small heat shock proteins. *Prion* **7**, 457-463
 58. Cashikar, A. G., Duennwald, M., and Lindquist, S. L. (2005) A chaperone pathway in protein disaggregation. Hsp26 alters the nature of protein aggregates to facilitate reactivation by Hsp104. *J Biol Chem* **280**, 23869-23875
 59. Haslbeck, M., Miess, A., Stromer, T., Walter, S., and Buchner, J. (2005) Disassembling protein aggregates in the yeast cytosol. The cooperation of Hsp26 with Ssa1 and Hsp104. *J Biol Chem* **280**, 23861-23868
 60. Doyle, S. M., Shorter, J., Zolkiewski, M., Hoskins, J. R., Lindquist, S., and Wickner, S. (2007) Asymmetric deceleration of ClpB or Hsp104 ATPase activity unleashes protein-remodeling activity. *Nat Struct Mol Biol* **14**, 114-122

61. DeSantis, M. E., Sweeny, E. A., Snead, D., Leung, E. H., Go, M. S., Gupta, K., Wendler, P., and Shorter, J. (2014) Conserved distal loop residues in the Hsp104 and ClpB middle domain contact nucleotide-binding domain 2 and enable Hsp70-dependent protein disaggregation. *J Biol Chem* **289**, 848-867
62. Jackrel, M. E., DeSantis, M. E., Martinez, B. A., Castellano, L. M., Stewart, R. M., Caldwell, K. A., Caldwell, G. A., and Shorter, J. (2014) Potentiated Hsp104 Variants Antagonize Diverse Proteotoxic Misfolding Events. *Cell* **156**, 170-182
63. Jackrel, M. E., and Shorter, J. (2014) Potentiated Hsp104 variants suppress toxicity of diverse neurodegenerative disease-linked proteins. *Disease Models & Mechanisms* **7**, 1175-1184
64. Jackrel, M. E., Tariq, A., Yee, K., Weitzman, R., and Shorter, J. (2014) Isolating Potentiated Hsp104 Variants Using Yeast Proteinopathy Models. *J Vis Exp* **93**, e52089
65. Jackrel, M. E., and Shorter, J. (2014) Reversing deleterious protein aggregation with re-engineered protein disaggregases. *Cell Cycle* **13**, 1379-1383
66. Jackrel, M. E., and Shorter, J. (2015) Engineering enhanced protein disaggregases for neurodegenerative disease. *Prion* **9**, 90-109
67. Jackrel, M. E., Yee, K., Tariq, A., Chen, A. I., and Shorter, J. (2015) Disparate Mutations Confer Therapeutic Gain of Hsp104 Function. *ACS Chem Biol* **10**, 2672-2679
68. Torrente, M. P., Castellano, L. M., and Shorter, J. (2014) Suramin inhibits Hsp104 ATPase and disaggregase activity. *PLoS One* **9**, e110115
69. Sweeny, E. A., DeSantis, M. E., and Shorter, J. (2011) Purification of hsp104, a protein disaggregase. *J Vis Exp* **55**, e3190
70. Werbeck, N. D., Schlee, S., and Reinstein, J. (2008) Coupling and dynamics of subunits in the hexameric AAA+ chaperone ClpB. *J Mol Biol* **378**, 178-190
71. Moreau, M. J., McGeoch, A. T., Lowe, A. R., Itzhaki, L. S., and Bell, S. D. (2007) ATPase site architecture and helicase mechanism of an archaeal MCM. *Mol Cell* **28**, 304-314
72. Sanchez, Y., and Lindquist, S. L. (1990) HSP104 required for induced thermotolerance. *Science* **248**, 1112-1115
73. Johnson, B. S., McCaffery, J. M., Lindquist, S., and Gitler, A. D. (2008) A yeast TDP-43 proteinopathy model: Exploring the molecular determinants of TDP-43 aggregation and cellular toxicity. *Proc Natl Acad Sci USA* **105**, 6439-6444
74. Johnson, B. S., Snead, D., Lee, J. J., McCaffery, J. M., Shorter, J., and Gitler, A. D. (2009) TDP-43 is intrinsically aggregation-prone, and amyotrophic lateral sclerosis-linked mutations accelerate aggregation and increase toxicity. *J Biol Chem* **284**, 20329-20339
75. Sun, Z., Diaz, Z., Fang, X., Hart, M. P., Chesi, A., Shorter, J., and Gitler, A. D. (2011) Molecular determinants and genetic modifiers of aggregation and toxicity for the ALS disease protein FUS/TLS. *PLoS Biol* **9**, e1000614
76. Gietz, R. D., and Schiestl, R. H. (2007) High-efficiency yeast transformation using the LiAc/SS carrier DNA/PEG method. *Nat Protoc* **2**, 31-34
77. Schirmer, E. C., Homann, O. R., Kowal, A. S., and Lindquist, S. (2004) Dominant gain-of-function mutations in Hsp104p reveal crucial roles for the middle region. *Mol Biol Cell* **15**, 2061-2072
78. Cashikar, A. G., Schirmer, E. C., Hattendorf, D. A., Glover, J. R., Ramakrishnan, M. S., Ware, D. M., and Lindquist, S. L. (2002) Defining a pathway of communication from the C-terminal peptide binding domain to the N-terminal ATPase domain in a AAA protein. *Mol Cell* **9**, 751-760
79. Outeiro, T. F., and Lindquist, S. (2003) Yeast cells provide insight into alpha-synuclein biology and pathobiology. *Science* **302**, 1772-1775
80. Cushman, M., Johnson, B. S., King, O. D., Gitler, A. D., and Shorter, J. (2010) Prion-like disorders: blurring the divide between transmissibility and infectivity. *J Cell Sci* **123**, 1191-1201
81. Ju, S., Tardiff, D. F., Han, H., Divya, K., Zhong, Q., Maquat, L. E., Bosco, D. A., Hayward, L. J., Brown, R. H., Jr., Lindquist, S., Ringe, D., and Petsko, G. A. (2011) A yeast model of FUS/TLS-dependent cytotoxicity. *PLoS Biol* **9**, e1001052

82. Schaupp, A., Marcinowski, M., Grimminger, V., Bosl, B., and Walter, S. (2007) Processing of proteins by the molecular chaperone Hsp104. *J Mol Biol* **370**, 674-686
83. Yu, A., Shibata, Y., Shah, B., Calamini, B., Lo, D. C., and Morimoto, R. I. (2014) Protein aggregation can inhibit clathrin-mediated endocytosis by chaperone competition. *Proc Natl Acad Sci U S A* **111**, E1481-1490
84. Auluck, P. K., Chan, H. Y., Trojanowski, J. Q., Lee, V. M., and Bonini, N. M. (2002) Chaperone suppression of alpha-synuclein toxicity in a Drosophila model for Parkinson's disease. *Science* **295**, 865-868
85. Takahashi, A., Hara, H., Kurahashi, H., and Nakamura, Y. (2007) A systematic evaluation of the function of the protein-remodeling factor Hsp104 in [PSI⁺] prion propagation in *S. cerevisiae* by comprehensive chromosomal mutations. *Prion* **1**, 69-77

FIGURE LEGENDS

Figure 1. Hsp104 hexamers must contain 2-3 A503V subunits for enhanced disaggregase activity in the absence of Hsp70. (A) Domain structure of Hsp104. N-terminal domain (purple), NDB1 (olive green), MD (orange), NBD2 (blue) and the C-terminal domain (red) are shown. Hsp104 mutations included in this study and their functional effects are also shown. Mutations affecting substrate binding are shown in mustard, while mutations affecting ATP binding and hydrolysis are shown in light blue. The potentiation mutation A503V is shown in pink. (B) Theoretical Hsp104 heterohexamer ensembles containing 0-6 WT subunits as a function of the fraction of WT subunit present. (C) Hsp104 was mixed in varying ratios with Hsp104^{A503V} to create heterohexamer ensembles. Luciferase disaggregation and reactivation activity was assessed in the absence of Hsp70 and Hsp40. Values represent means \pm S.E.M. ($n = 3$). Theoretical curves are shown to illustrate the predicted result when 1-6 WT subunits are needed to inactivate the Hsp104^{A503V} hexamer. (D) The data plotted in (C) is replotted. Theoretical curves are shown where adjacent pairs of A503V:A503V or A503V:WT subunits confer hexamer activity, while adjacent WT subunits are inactive. Each adjacent A503V:A503V pair has an activity of 1/6. Adjacent A503V:WT pairs have a repressed activity (r), and the effect of various r values are depicted.

Figure 2. Hsp104^{A503V} disaggregase activity is severely impaired by the Y257A mutation and ablated by the Y662A mutation. (A) Hsp104 mutants (0.25 μ M monomer) were incubated for 10 minutes with ATP (1mM). Average absorbance from a no enzyme control reaction was subtracted from raw absorbance values. Resulting absorbance values were normalized to the average absorbance yielded by Hsp104^{WT}. Values represent means \pm S.E.M ($n = 16-48$). A one-way ANOVA with the post-hoc Tukey's multiple comparisons test (* denotes $p < 0.05$; ** denotes $p < 0.01$). (B) Urea-denatured firefly luciferase aggregates were incubated for 90 minutes at 25°C with Hsp104 (1 μ M hexamer) plus ATP. Luciferase reactivation was then determined and normalized to Hsp104^{WT} disaggregase activity. Values represent means \pm S.E.M ($n = 6-90$). (C) Reactions were performed as in (B) except that 1:1 mixtures of ATP and ATP γ S replaced ATP. Values represent means \pm S.E.M ($n = 6-84$). (D) Reactions were performed as in (B) except that Hsp70 (1 μ M) and Hsp40 (1 μ M) were added. Values represent means \pm S.E.M ($n = 6-84$).

Figure 3. Hsp104^{A503V}-mediated rescue of yeast proteinopathy models is severely impaired by the Y257A mutation and ablated by the Y662A mutation. $\Delta hsp104$ yeast integrated with genes encoding (A) α -syn, (C) FUS, or (E) TDP-43 were transformed with the indicated Hsp104 variants or empty vector control. Strains were serially diluted five-fold and spotted on glucose (off) or galactose (on) media. (B), (D), and (F) Strains from (A), (C), and (E) respectively were induced, lysed, and immunoblotted. 3-Phosphoglycerate kinase (PGK) was used as a loading control. Figures shown are representative of at least 3 independent trials.

Figure 4. Hsp104^{A503V} requires a lower proportion of ATP γ S for maximal disaggregase activity in the absence of Hsp70 compared to Hsp104. (A, B) Urea-denatured firefly luciferase aggregates were incubated for 90 minutes at 25°C with the indicated Hsp104 variant (1 μ M hexamer) in the presence of the indicated amounts of ATP and ATP γ S (total nucleotide concentration was kept constant). Values represent means \pm S.E.M ($n = 4-5$). (A) All data points were normalized to the maximum refolding activity of WT Hsp104. (B) All data points were normalized to the maximum refolding activity for a given Hsp104 mutant.

Figure 5. A potentiated Hsp104 variant can overcome deficits in ATP hydrolysis at NBD1 or NBD2 *in vitro*. (A) Hsp104^{A503V} mutants (0.25 μ M monomer) were incubated for 10 minutes with ATP (1mM). Average absorbance from a no enzyme control reaction was subtracted from raw absorbance values. Resulting absorbance values were normalized to the average absorbance yielded by Hsp104^{WT}. Values represent mean \pm S.E.M ($n = 16-48$). A one-way ANOVA with the post-hoc Tukey's multiple comparisons test (* denotes $p < 0.05$; ** denotes $p < 0.01$). (B) Urea-denatured firefly luciferase aggregates

were incubated for 90 minutes at 25°C with Hsp104 (1µM hexamer) plus ATP. Luciferase reactivation was then determined and normalized to Hsp104^{WT} disaggregase activity. Values represent mean ±S.E.M (*n*=6-78). **(C)** Reactions were performed as in **(B)** except that 1:1 mixtures of ATP and ATPγS replaced ATP. Values represent mean ±S.E.M (*n*=6-72). **(E)** Reactions were performed as in **(B)** except that Hsp70 (1µM) and Hsp40 (1µM) were added. Values represent mean ±S.E.M (*n*=6-72).

Figure 6. ATPase activity at NBD1 or NBD2 in Hsp104^{A503V} is sufficient to sustain potentiation in yeast proteinopathy models. *Δhsp104* yeast integrated with genes encoding **(A)** α-syn, **(C)** FUS, or **(E)** TDP-43 were transformed with the indicated Hsp104 mutants or control. Strains were serially diluted five-fold and spotted on glucose (off) or galactose (on) media. **(B)**, **(D)** and **(F)** Strains from **(A)**, **(C)** and **(E)** respectively were induced for 5 or 8 hours, lysed, and immunoblotted. 3-Phosphoglycerate kinase (PGK) was used as a loading control. Figures shown are representative of at least 3 independent trials.

Figure 7. Summary of key mechanistic insights into Hsp104 potentiation.

Table 1. Summary of Hsp104 variants and their ATPase and luciferase reactivation activities under the conditions tested in this paper. Numbers for partial or increased activities are noted. Numbers in blue represent a decrease in activity with respect to Hsp104^{WT}, while numbers in red represent increased activity.

TABLES

Table 1

Hsp104 Mutant	ATPase Activity	Refolding Activity		
		ATP	1:1 ATP/ATP γ S	Hsp72+ Hdj1
WT	1.00	1.00	1.00	1.00
Y257A	1.09	0.97	0.04	0.15
T317A	0.64	1.92	1.14	0.93
A503V	1.18	32.76	0.13	0.51
Y662A	1.14	1.12	0.01	0.00
N728A	0.67	352.22	0.17	1.87
K218T K620T (DWA)	0.08	0.44	0.00	0.01
E285Q E687Q (DWB)	0.04	0.24	0.00	0.01
Y257A Y662A	1.37	0.47	0.02	0.01
Y257A A503V	1.15	2.02	0.09	0.07
T317A A503V	0.81	54.79	0.16	0.43
Y662A A503V	1.42	0.75	0.01	0.00
N728A A503V	0.97	571.10	0.01	2.36
K218T A503V K620T (DWA A503V)	0.07	0.53	0.00	0.01
E285Q A503V E687Q (DWB A503V)	0.08	0.34	0.00	0.01
Y257A A503V Y662A	0.77	0.40	0.00	0.01

FIGURES

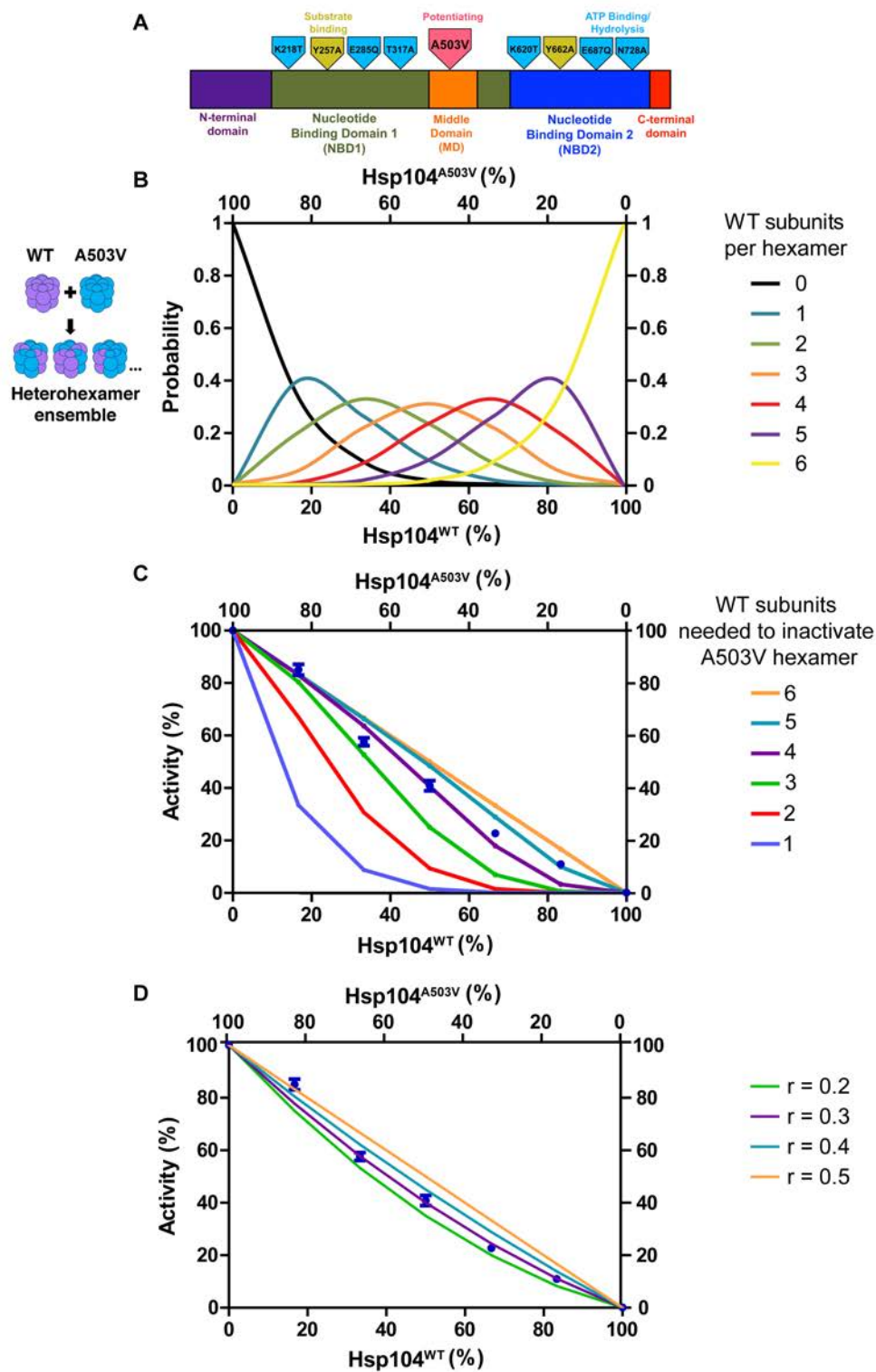


Figure 1.

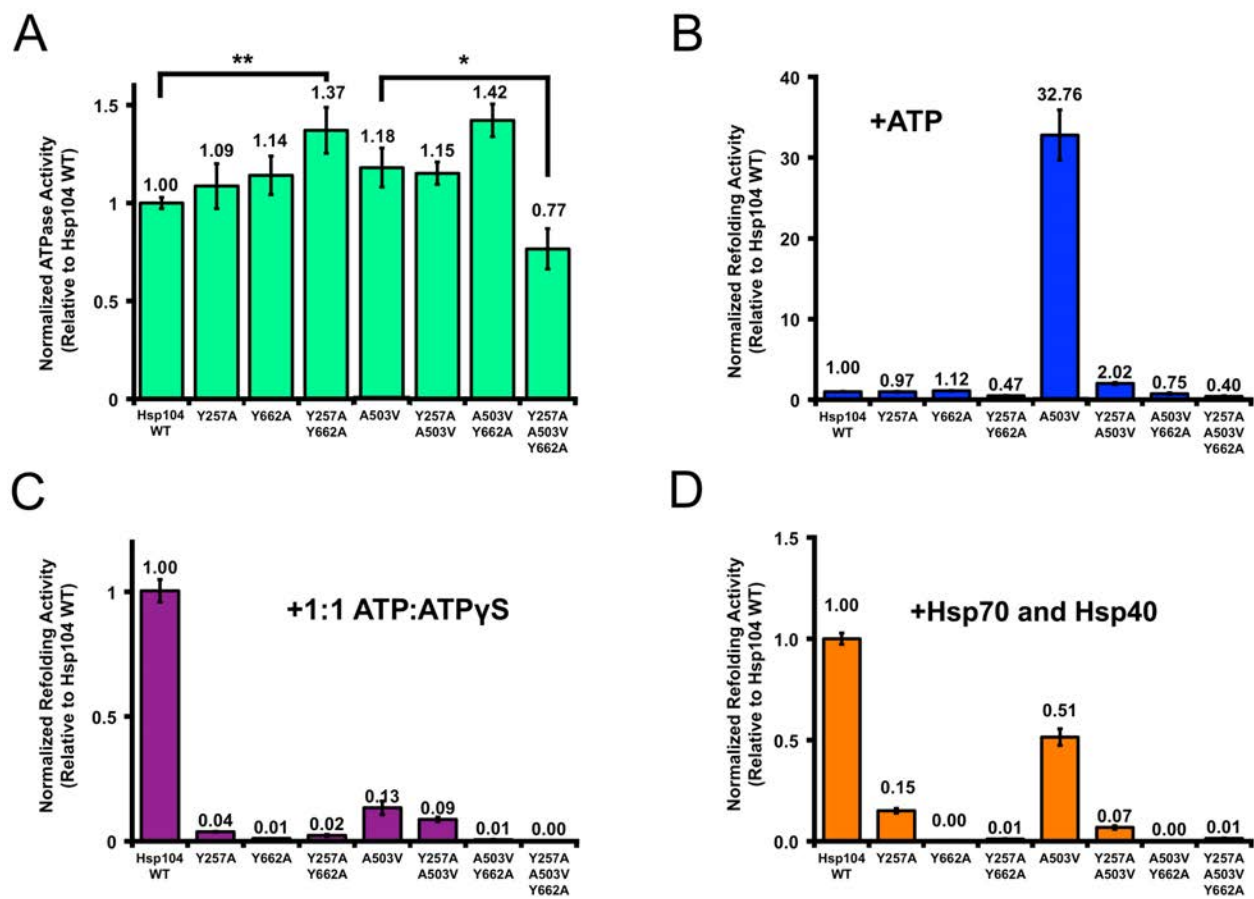


Figure 2.

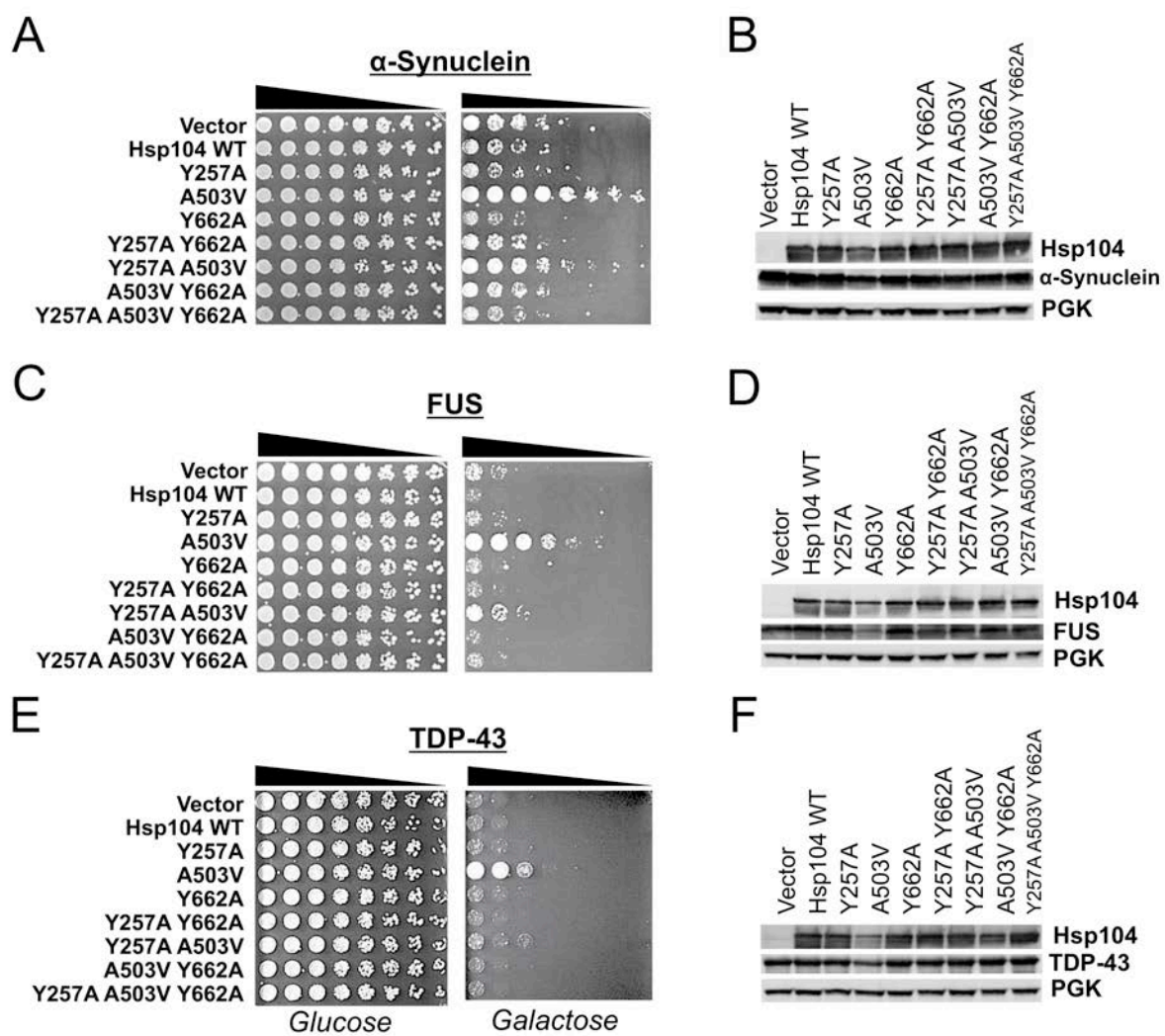


Figure 3.

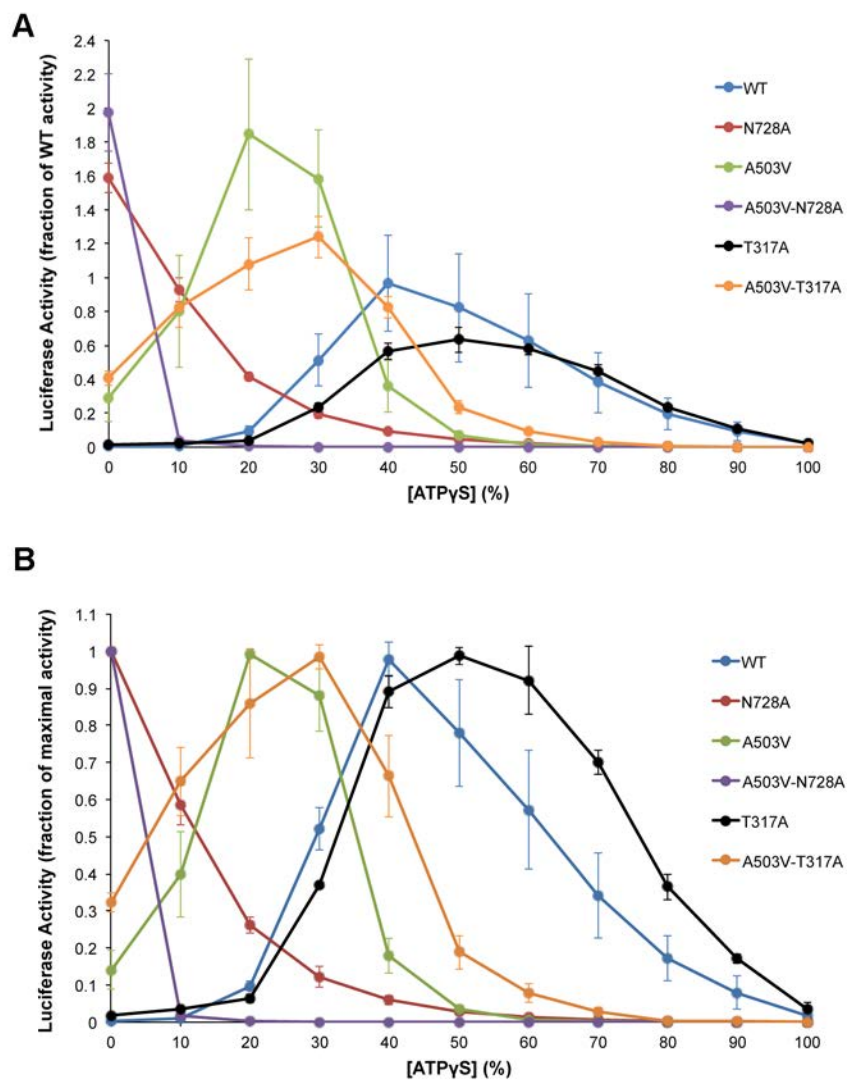


Figure 4.

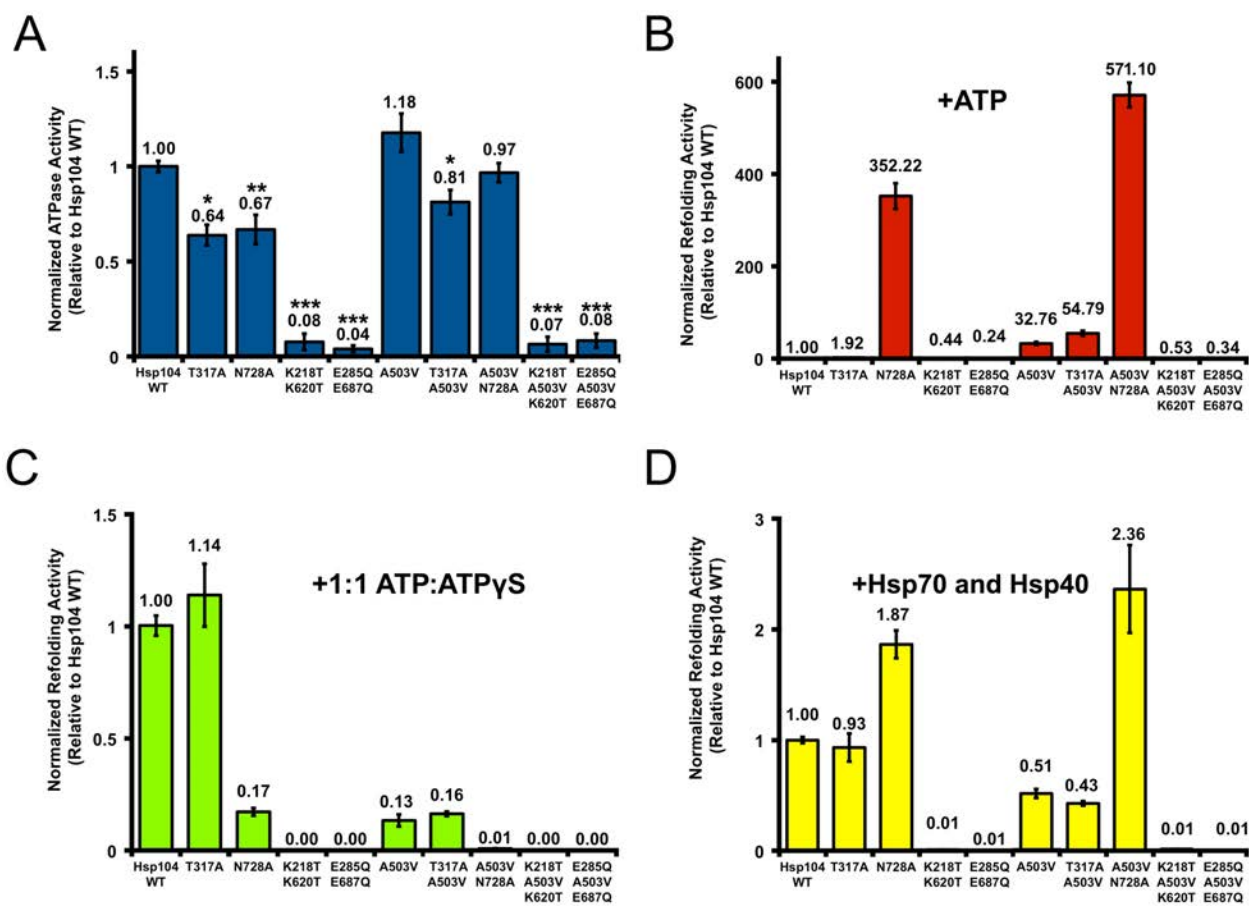


Figure 5.

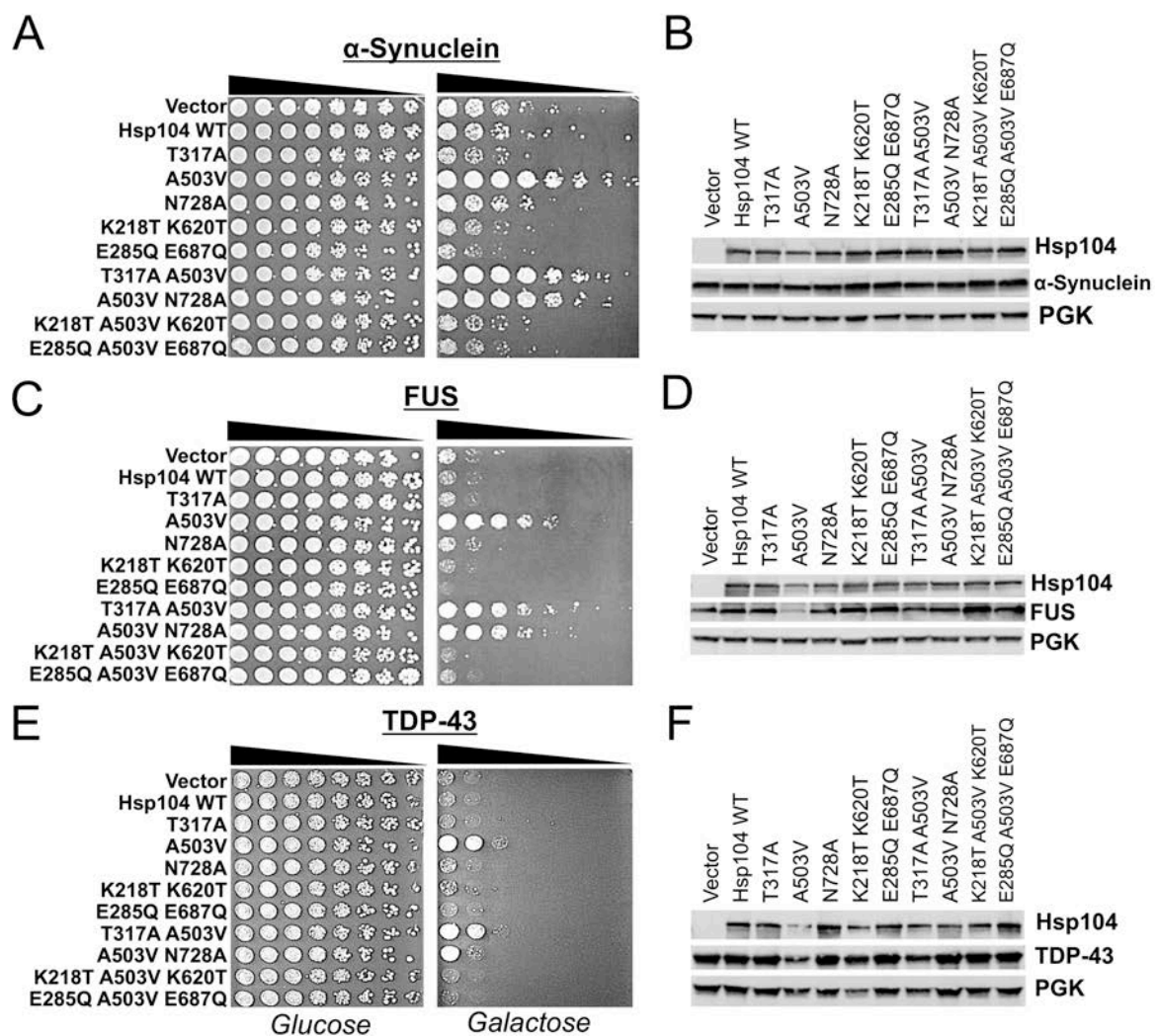


Figure 6.

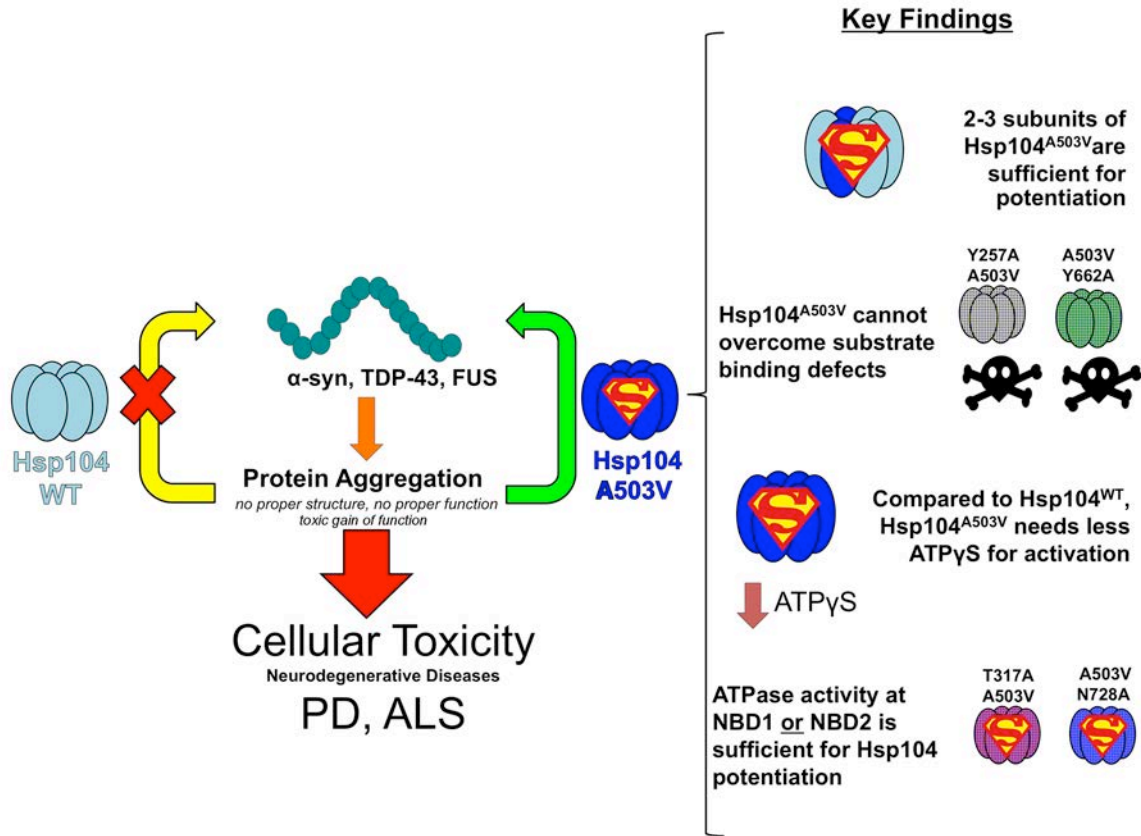


Figure 7.

Mechanistic Insights Into Hsp104 Potentiation

Mariana P. Torrente, Edward Chuang, Megan M. Noll, Meredith E. Jackrel, Michelle S. Go
and James Shorter

J. Biol. Chem. published online January 8, 2016

Access the most updated version of this article at doi: [10.1074/jbc.M115.707976](https://doi.org/10.1074/jbc.M115.707976)

Alerts:

- [When this article is cited](#)
- [When a correction for this article is posted](#)

[Click here](#) to choose from all of JBC's e-mail alerts

This article cites 0 references, 0 of which can be accessed free at
<http://www.jbc.org/content/early/2016/01/08/jbc.M115.707976.full.html#ref-list-1>